PROCEEDINGS, Fifteenth Workshop on Geothermal Reservoir Engineering
Stanford University, Stanford, California, January 23-25, 1990
SGP-TR-130

SEISMIC SURVEY AT THE SOULTZ HDR GEOTHERMAL ENERGY PROJECT

D. LE MASNE(*), A. BEAUCE(*), H. FABRIOL(*)
C. CAVOIT(**), P. MECHLER (***), X. CHEN (*)

* BRGM/IMRG - BP 6009 - 45060 Orléans Cedex 2 - FRANCE
** CNRS/CRG Garchy - 58150 Pouilly/Loire- FRANCE
*** UNIVERSITE DE PARIS VI - Laboratoire de Géophysique Appliquée 4 Pl. Jussieu - 75230 PARIS Cedex 5 - FRANCE

ABSTRACT

A French-German Hot Dry Rock project, co-sponsored by the European Community, is underway at Soultz (Alsace, France). Borehole GPK1, drilled in 1987 down to 2000 m (600 m of granite under a 1400-m-thick sedimentary cover) reached a 140°C bottom temperature.

Major fractures were discovered or pointed out by an active VSP seismic survey (VSP, Offset VSP, Walk-Away) and by the reprocessing of already-existing Seismic Reflection profiles. A velocity model was derived from the VSP survey and from shots in GPK1.

A 3-day hydraulic test undertaken at the bottom of GPK1 was surveyed by a seismic network consisting of 3-D probes cemented at the bottom of 3 neighbouring observation boreholes.

Despite a rather low flow-rate (3.3 l/s), 58 seismic events were recorded all over the stimulation test. Two main active zones were observed: one lies close to the stimulation chamber; the second one, some 100 m down, can be related to a reflector visible on one of the re-processed Seismic Reflection profiles. These two active zones could be connected through a subvertical fault pointed out by the active seismic survey.

INTRODUCTION

Hot Dry Rock geothermal energy projects began at Los Alamos (USA) and Camborne (UK) in the early 1970's. In both cases, a monitoring of the microseismicity induced in the rock by hydraulic stimulation was very helpful in defining the stimulated regions and reservoir growth (Baria, R. et al., 1989 ; Mock, J., 1989).

The HDR site of Soultz, in Alsace (northeastern France), was chosen in 1986 on the western side of a very large thermal anomaly which extends over about 4000 km² in the Rhine graben (Figure 1). This site overlaps the old Pechelbronn oil-field. This explains the availability of 60 deep wells drilled in the early 1950's and the existence of several Seismic Reflection profiles carried out by TOTAL in 1984.

Major faults dipping 60° W affect the thick sedimentary cover (1400 m) and the granite horst underneath (Cautru J.P., 1989). Borehole GPK1 reaches temperatures of 125°C at the top of the granite and 140°C at total depth (Kappelmeyer, O., Gérard, A., 1989).

A rather long (some weeks) hydraulic stimulation test had been first planned in GPK1 at different depths over short sections of the well.

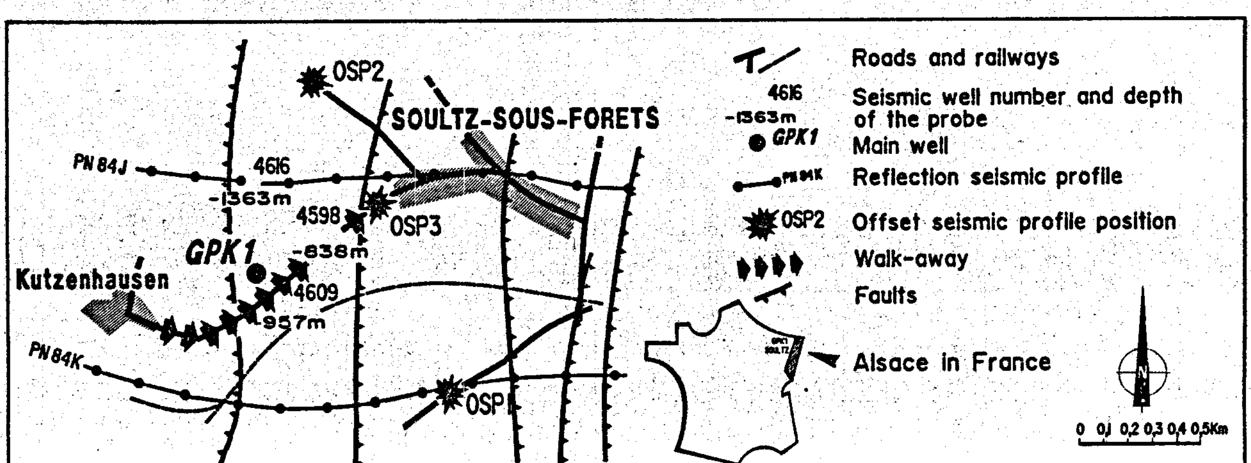

Figure 1 - Location map of the project

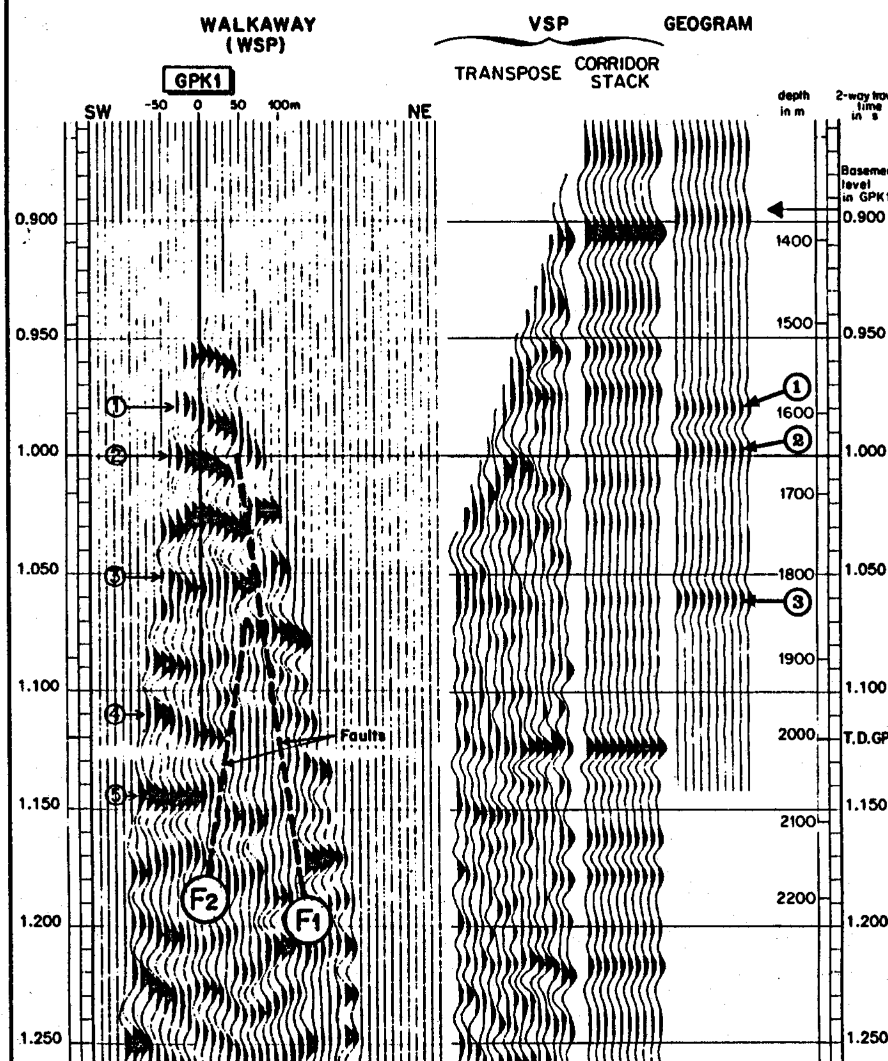

Figure 2 - Comparison of WSP and VSP seismic sections, and GEOGRAM

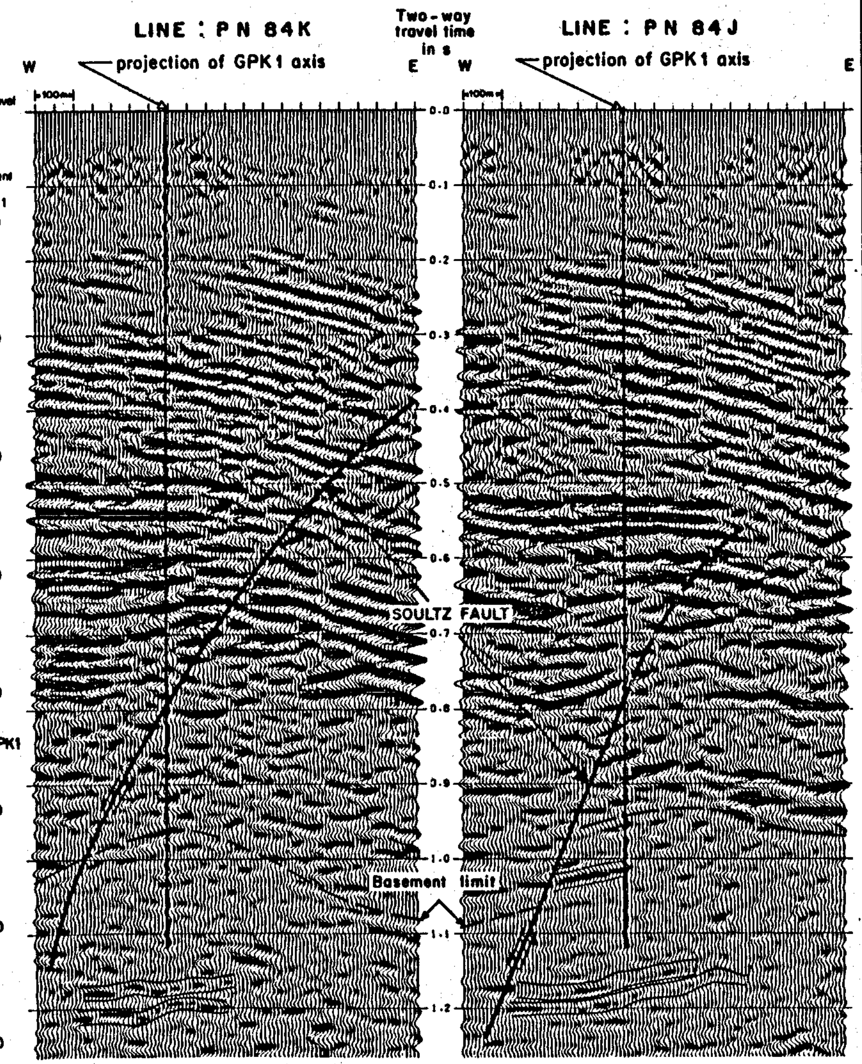

Figure 3 - Migrated seismic sections of lines PN 84J and PN 84K

To monitor the site during this hydraulic experiment, three old oil wells (4616, 4609, 4598, see Figure 1) were successfully recovered in 1987 in the vicinity of the main well GPK1 and instrumented with three-directional permanent seismic probes cemented at their bottom.

Before any stimulation, an active VSP seismic survey was carried out in October 1988 in order to:

- better define the extensions of the fractured zones around GPK1,
- give a velocity model allowing an accurate location of the seismic events to be recorded during the stimulation experiment.

This VSP survey was complemented by shots in GPK1, using Schlumberger's Core Sample Taker (CST) as a source. During all these operations the downhole seismic probes were operational and the signals recorded and analysed.

A re-interpretation of the TOTAL Seismic Reflection profiles (lines PN 84J and PN 84K, see Figure 1) emphasizing the granite section, was undertaken to correlate the structures observed in the vicinity of GPK1 with the granite sections 500 m south and north of GPK1.

Unexpected problems with the packers at high temperature reduced the expected duration of the stimulation experiment to a 3-day test over only a 30-m-long section of GPK1 (1970-2000 m). Despite these inconveniences, 58 seismic events were recorded and the bigger ones were located using the velocity model derived from the active seismic survey.

The results of the active seismic survey and of the seismic monitoring of the stimulation experiment will be described successively in this paper.

ACTIVE SEISMICS

VSP survey

The different field operations carried out by Schlumberger and by IMRG were the following (Figure 1):

- a VSP (Vertical Seismic Profile) along GPK1: 25 receiver levels (spacing 30 m) between 1250 and 1970 m (+ 6 check shots at 100, 300, 500, 700, 900 and 1050 m);
- 3 OSP (Offset VSP) with source offset between 500 and 900 m and 17 receiver levels every 30 m between 1250 m and 1730 m in GPK1;
- a 1-km-long WSP (Walk-Away Seismic Profile) along the NE-SW road joining boreholes GPK1 and 4598, with 26 surface sources every 40 m and 5 receiving levels every 25 m in GPK1 between 1425 and 1525 m depth;

The source used for VSP surveys was a Vibroseis (3 sweeps per point, transmission bandwidth 6-90 Hz).

Figure 2 is a comparison of three kinds of seismic sections (two-way time on all verticals):

- the Walk-Away VSP (WSP) obtained after waveshaping deconvolution and NMO (Normal Move-Out) corrections using a non-dipping model with velocities consistent with the Sonic log measurements;
- the Transpose (extension away from the well) and the Corridor Stack (vicinity of the well) of the VSP;
- the GEOGRAM (Schlumberger's trademark) directly calculated from the density and sonic logs performed just after the drilling of GPK1.

We first looked for reflectors with reverse polarity on the GEOGRAM, knowing that fractured zones are marked by a decrease in velocity and density causing reflections of seismic energy with opposite sign. Three main events (1, 2, 3, in Figure 2) of this type were found in the granite sections of the GEOGRAM, and of the WSP and VSP (except event 2) at 1590, 1640 and 1825 m (980, 1000, 1060 ms). They were well correlated with important altered and fractured zones observed by the analysis of cuttings and by logging methods (Genter, A., 1989). The third event (1060 ms) corresponds to the biggest water productive zone.

Three more events appeared on the WSP at 1530, 1730 and 1910 m (955, 1025 and 1090 ms), and for two of them on the VSP, without any corresponding event on the GEOGRAM. Events due to dipping fractures wich do not necessarily intersect GPK1 might be an explanation of this last point.

Two strong reflectors (4 and 5, in Figure 2) were also observed mostly on the south-western part of the WSP, starting at GPK1's bottom (1120 ms) and some 100 m down it (1145 ms). These reflectors could be linked to the stimulated zones described further on.

Two other major structures appeared on the WSP:

- a discrepancy in the reflections for horizontal offsets varying from +50 m to 130 m NE of GPK1, which can also be noticed on the OSP1 and OSP3 seismic sections. This could be due to a fault (F1) dipping 60 to 70° NE located some tens of meters east of GPK1 and visible in the granite between 1000 and 1200 ms (1650 and 2200 m depth);
- an interruption in the reflections for offsets varying from +60 m to 0 m between 1070 and 1180 ms (1850 and 2150 m depth), which could correspond to another fault (F2) dipping SW and crossing the axis of GPK1 some 100 m beneath its bottom.

Re-processing the Seismic Reflection profiles

Figure 3 shows a part of the migrated sections of lines PN 84J and PN 84K, using a velocity model deduced from a structural interpretation of the whole area (Cautru, J.P., 1989) and from the active seismic survey in GPK1.

On line PN 84K, sited 500 m south of GPK1, the basement is met at 975 ms instead of 895 ms in GPK1, that is a structural 80 ms difference. Two well-defined reflectors intersect the projection of the GPK1 axis at 1175 and 1200 ms. Taking into account the 80 ms difference, it is possible to correlate these reflectors with the events found on the VSP and the WSP at 1090 and 1120 ms respectively.

On lines PN 84J, sited 400 m north of GPK1, the basement is met at 950 ms, that is a 55 ms difference with GPK1's case. Three reflectors appear between 950 and 1220 ms. The first one, at 1020 ms, could correspond to the thick fractured zone at 1590-1640 m in GPK1. The two other zones, at 1160 and 1180 ms, correspond roughly to reflectors n° 4 and 5 noted on the VSP and the WSP at 1120 and 1145 ms. Given the relatively long distances between both sections and GPK1, these correspondances are only assumptions at that stage.

Coherency filters were applied to the migrated sections in order to find the better dip of the oblique reflectors. Good coherencies were found for dips of 35-45° West, which agrees with the main trend of the western flank of the Soultz horst.

Deep shots and velocity model

The tabular velocity model used to locate the stimulated events was derived from the combination of:

- Sonic-log velocities (corrected, after the VSP results, for the usual drift between sonic and seismic travel-times);
- Transit times for shots fired inside GPK1 at different levels, and recorded on the IMRG downhole network.

Depth (m)	Layer		Vp (m/s)	Vs (m/s)	Vp/Vs
860	Muschel-kalk	1	3620	2070	1.750
		2	3650 ± 100	-	-
		3	3620	2150	1.685
900	Bunt-sandstein	1	4410	2520	1.750
		2	4330 ± 30	-	-
		3	4330	2570	1.685
1376	Granite	1	5640	3250	1.735
		2	5680	3370	1.685
		3	5680	3370	1.685
2000					

Table 1 - Velocity estimates from corrected Sonic Log (1) and Deep shots (2) Final velocity model chosen (3)

Table 1 gives the velocities obtained by the two approaches (1: Corrected Sonic velocities, 2: Shot velocities) for the 3 main layers between 860 m (probe 4598) and 2000 m depth, and the final velocity model chosen (3: final model) to locate the events.

Twenty-one CST (Core Sample Taker) shots, and two shots with classic explosives, fired between 1400 and 2000 m depth in GPK1, were recorded on our three downhole probes to complete and test the first velocity model obtained by the corrected Sonic log. P- and S-wave onsets were clear enough on probe 4616 (z = 1400 m) to calculate reliable P- and S-wave velocities in the granite (see Table 1).

The P-wave velocities obtained in the granite by the two methods are quite comparable (less than 1 % difference). The Vp/Vs ratios, however, are rather different (1.735 versus 1.685); this difference is probably due to the limited radius of investigation of the Sonic tool around the borehole. For our final model, in the granite, we chose the Vp/Vs value given by the shots, which better integrates velocities all along the raypath.

The poor quality of the P- and S-wave onsets of the shots on the uppermost probes (4598 and 4605) was improved by stacking and cross-correlation techniques, leading to reliable P-wave velocities in the Buntsandstein and in the Muschelkalk (greater uncertainty in this last case, see Table 1). Once again, these P-wave results are very comparable to those given by the corrected Sonic logs. No reliable S-wave velocities could be derived, from these shots, for the two sedimentary layers. To get S-wave velocities in these layers, we merely applied the Vp/Vs ratio obtained in the granite (1.685) to the corresponding P-wave velocities obtained with the shots.

Figure 4 shows the final velocity model and the location of the observation boreholes with regard to GPK1.

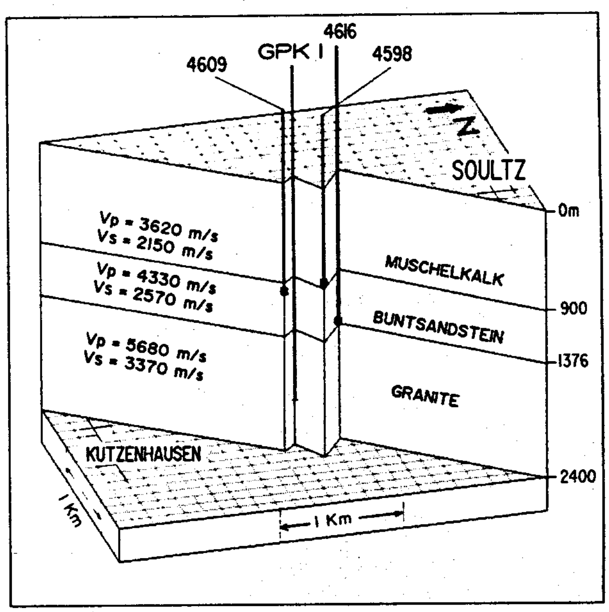

Figure 4 - Velocity model

SEISMIC SURVEY DURING STIMULATION IN GPK1

Acquisition network and data processing

The seismic network designed and installed by IMRG consists of three-directional probes, especially designed to withstand the rough temperature (100 to 125°C) and corrosion conditions, and cemented at the bottom of three observation boreholes.

Only one (4616) of these three boreholes reached the granite (Figure 4) and the probes were thus rather far away (750 to 1200 m) from the stimulated zone at GPK1's bottom. Every probe was equipped with 3 high-temperature geophones (2 horizontal and 1 vertical) with a 20 Hz resonance frequency. Their sensitivity at 30 Hz (0.4 V/inch/s) decreases only by 15% at 300 Hz and 35% at 1500 Hz.

The acquisition software allowed continuous monitoring of the 9 channels of the network and detection of the seismic events recorded at a sampling rate of 8000 Hz per channel. The detection algorithm used, was based on the ratio of a short-term average absolute value of the signal amplitude over a long-terme one. Channels used for detection during the stimulation were those of the deepest probe (4616). Each time a detection was declared, the system stored 1 second on the 9 channels (300 ms before the detection, 700 ms after) and displayed the signal of one channel on the screen.

Seismicity induced by the stimulation experiment

A total amount of 524 m^3 of water was injected between 14 december at 10 a.m. and 16 december at 11 p.m, over a 30-m-long vertical section of GPK1 well, between 1970 m and the bottom. The water-flow was nearly constant (3.3 l/s) except during short periods of several minutes at the beginning. The well-head pressure reached a maximum of 82 bars, corresponding to 47 bars at total depth.

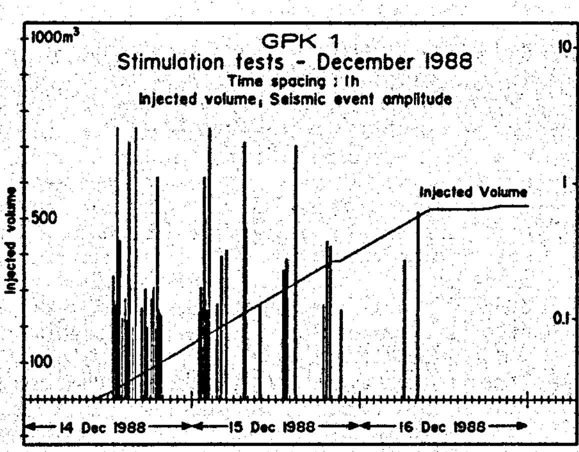

Figure 5 - Time of occurrence and amplitudes of the seismic events recorded on probe 4616 during stimulation

Fifty-eight microseims were induced by the stimulation (Figure 5) and no event was recorded during the shut-in period (Beauce, A., et al., 1989). The first event occurred only after 2 hours of injection, that is for an injected volume of 25 m^3.

Figure 5 illustrates the chronological variations of the maximum amplitude on channel X of probe 4616 for the 58 recorded events. The decrease of the seismicity (rate of events) and of the amplitude with time can be interpreted as an evolution of the system towards a new steady state.

Results of the spectral analysis carried out on the 58 events using an FFT algorithm on 512 samples (time window of 64 ms) show that power spectra are very similar for all the events, for a given channel of a given probe. As expected, the P-wave spectral content is higher (150-300 Hz) for the probe sited in the granite than for the shallower ones (40-200 Hz).

A bi-modal distribution (Figure 6) of the differences (Ts-Tp) between S and P arrival times on probe 4616 could be observed for the 58 events: 13 events with (Ts-Tp) between 91 and 95 ms, and 39 ones between 99 and 109 ms (Figure 6). This corresponds to at least two focal zones.

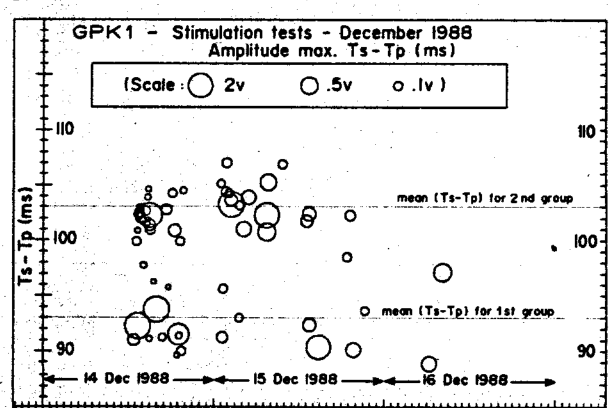

Figure 6 - Chronological display of the S-P arrival time differences and of the maximum amplitudes on probe 4616 for the 58 events

Although seismic activity starts and continues simultaneously for the two families, the seismic-energy-release patterns are rather different. For the group closest to 4616, the events of higher magnitudes occur at the beginning of the microseismic emission (Figure 6), whereas for the other group, the higher magnitudes are observed after 16 h of pumping, which can be due to the propagation delay of the pressure.

This last trend supports the assumption of the existence of two families that are not linked to the same fracture. But, even if they are distinct, they where affected by the same mechanism, since their signatures are similar for a given probe.

Location of the events

Only 12 events out of the whole data set were selected to be localized, as the other ones did not allow an accurate enough P- or S- wave picking on the seismograms recorded by the probes sited in the sedimentary cover.

Using both P- and S-wave arrival times observed on probe 4616, and the defined velocity-model (Figure 4), we calculated the origin time of the events. A 3-D grid (mesh size 20 m) of points surrounding GPK1's bottom was defined and, taking into account ray refractions at the different interfaces, theoretical P- and S-wave propagation times from the nodes of this grid to each of the 3 probes were calculated. Intersections of the surfaces representing the possible source locations compatible with the observed propagation times on each probe for both P and S waves, define a narrow zone from where the event originates.

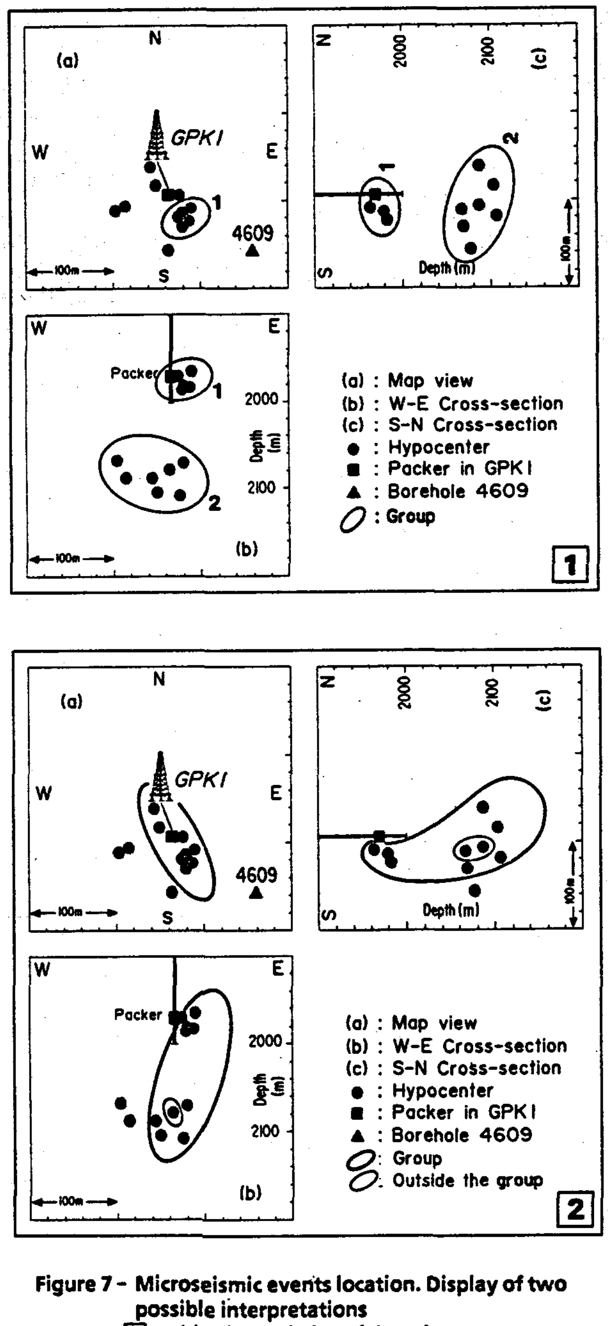

Figure 7 - Microseismic events location. Display of two possible interpretations
1 subhorizontal plane (above)
2 subvertical plane (below)

Figure 7 displays the projections of the 12 calculated hypocenters on three orthogonal planes (a horizontal and two E-W and N-S vertical ones passing by GPK1). Two interpretations can be given following the way the hypocenters are grouped together.

In the first interpretation (upper part of Figure 7), one can distinguish two active zones: the first one(1) groups 5 events clustered close to GPK1; the second one(2) gathers the 7 other events, more widely spread out, on a subhorizontal plane at 2090 m depth (see projections on the 2 vertical planes in Figure 7). In this interpretation, which takes into account all the calculated hypocenters, the second active zone may be related to a reflector (fracture, crushed zone?) observed on the WSP (event 5 in Figure 2) and on the re-processed PN 84J Seismic Reflection profile.

The second interpretation groups 9 events together, along a subvertical plane orientated N 160-170°. This interpretation, although disregarding 3 events whose origin cannot be directly related to a seismic feature, is in better accordance with fault F2 observed on the WSP survey, which could connect the two active zones at 2000 and 2100 m depth. Furthermore this interpretation is more compatible with the maximal-horizontal- stress component (fracture development easier along this direction) deduced by BHTV data analysis (N170°) and by in situ stress measurements (N145°).

In any case, the few reliable data obtained in this short experiment cannot enable us to go further in these assumptions. To estimate the precision of the resulting locations, observed arrival times were artificially disturbed by ± 1 ms, successively on the different probes, leading to a k 15 m uncertainty around the initial location. The influence of different Vp/Vs ratios (1.66 and 1.73), for the sedimentary layers only, was also modelled, leading to a spatial uncertainty of ± 15 m in the final locations. The combined location error is of the order of ± 30 m.

CONCLUSIONS

Despite a rather low flow-rate (3.3 l/s) and a low bottom-hole pressure (47 bars), a notable seismicity was recorded during the stimulation experiment undertaken at Soultz in December 1988. This seismicity decreased with time (event-rate and magnitudes), indicating that the system had reached a new steady state. These results have been made possible by the proper design of specific, permanently-installed, geophones suited to the rough downhole temperature and corrosion conditions.

Location results indicate that two zones of weakness were concerned during the experiment: a first one close to the top of the injection zone in GPK1 borehole, and another one 100 m deeper than the bottom of the hole, which could be related to a seismic feature pointed out by the VSP survey and by the reprocessing of an already-existing Seismic Reflection profile. These two active zones could have been connected through a N 160-170° subvertical fracture pointed out during the Walk-Away experiment.

The feasibility of such a seismic array to monitor artificially created or re-opened fractures is confirmed by the present work, but these results also pointed out the necessity of more than three observation boreholes. To obtain more reliable results and to be able to use all the data recorded on the network, these probes must be furthermore sited inside the granite where attenuation effects are less dramatic. Further stimulation operations monitored with a denser seismic observation network must be planned in the second scientific phase of the Soultz project (1990-1991), before any industrial exploitation.

ACKNOWLEDGEMENTS

This work has been financially supported by the European Economic Community, the A.F.M.E. (Agence Française pour la Maîtrise de l'Energie), and B.R.G.M.

REFERENCES

BARIA, R., GREEN, A.S.P. (1989) - Microseismics: a key to understanding reservoir growth. International HDR Conference, Camborne (UK), 27-30 June 1989.

BEAUCE, A., FABRIOL, H., LE MASNE, D. (1989) - Seismicity induced during a hydraulic stimulation at the Soultz-sous-Forêts HDR Geothermal Energy Project. 59th annual international SEG meeting, Dallas, Nov. 1989, Vol. I, pp. 241-243.

BEAUCE, A., FABRIOL, H., LE MASNE, D., CAVOIT, C., MECHLER, P., CHEN, X. (1989) - Seismic monitoring on the Soultz site. International HDR Conference, Camborne (UK), 27-30 June 1989.

CAUTRU, J.P. (1989) - Coupe géologique passant par le forage GPK1 calée sur la sismique reflexion. IMRG document.

GENTER, A. (1989) - Géothermie Roches Chaudes Sèches. Le granite de Soultz-sous-Forêts. Fracturation naturelle, altérations hydrothermales et interactions eau-roche. Thesis, University of Orleans, 30 October 1989.

KAPPELMEYER, O., GERARD, A. (1989) - The European geothermal project at Soultz-sous-Forêts. Proceedings of the 4th International seminar on the results of E.C. geothermal energy research and demonstration. Florence 27-30 April 1989. pp. 283-334.

MOCK, J. (1989) - The U.S. Hot Dry Rock program. International Hot Dry Rock Geothermal Energy Conference, Camborne (U.K.), 27-30 June 1989.